Research article

14-3-3ζ negatively regulates mitochondrial biogenesis in GBM residual cells

Jacinth Rajendra [a,b,1], Atanu Ghorai [a,1], Shilpee Dutt [a,b,*]

[a] Shilpee Dutt Laboratory, Advanced Centre for Treatment, Research and Education in Cancer (ACTREC), Tata Memorial Centre, Navi Mumbai, India
[b] Homi Bhabha National Institute, Training School Complex, Anushakti Nagar, Mumbai, 400085, India

HIGHLIGHTS

- 14-3-3ζ is up-regulated in residual disease cells of GBM.
- 14-3-3ζ knockdown radiosensitizes GBM cells.
- 14-3-3ζ knockdown increases MNGCs formation and senescence in residual cells.
- 14-3-3ζ negatively regulates mitochondrial biogenesis of residual disease cells.
- Novel interacting partners of 14-3-3ζ from residual cells are involved in cellular metabolism.

ARTICLE INFO

ABSTRACT

Glioblastoma (GBM) is the most lethal primary brain tumour with a median survival of only 15 months. We have previously demonstrated the generation of an *in vitro* therapy resistance model that captures the residual resistant (RR) disease cells of GBM post-radiation. We also reported the proteomic landscape of parent, residual, and relapse cells using iTRAQ based quantitative proteomics of glioma cells. The proteomics data revealed significant up-regulation (fold change >1.5) of 14-3-3ζ, specifically in GBM RR cells. This was further confirmed by western blots in residual cells generated from GBM cell lines and patient sample-derived short-term primary culture. ShRNA-mediated knockdown of 14-3-3ζ radio-sensitized GBM cells and further stimulated therapy-induced senescence (TIS) and multinucleated giant cells (MNGCs) phenotype in RR cells. Intriguingly, 14-3-3ζ knockdown residual cells also showed a significantly higher number of mitochondria and increased mtDNA content. Indeed, *in vitro* GST pull-down mass spectrometry analysis of GST tagged 14-3-3ζ from RR cells identified novel interacting partners of 14-3-3ζ involved in cellular metabolism. Taken together, here we identified novel interacting partners of 14-3-3ζ and proposed an unconventional function of 14-3-3ζ as a negative regulator of TIS and mitochondrial biogenesis in residual resistant cells and loss of which also radio-sensitize GBM cells.

1. Introduction

Glioblastoma (GBM) is the most lethal primary brain tumour. Despite aggressive radio-chemo therapy, GBM shows dismal median survival of 15 months mainly due to intrinsic resistance of heterogeneous GBM cells to therapy [1]. Furthermore, the lack of repeat biopsies of brain tumour patients post-therapy makes it difficult to understand the molecular mechanism of resistance. Therefore, we established an *in vitro* therapy-resistant GBM model derived from GBM cell lines and primary cultures from patient samples that recapitulate the clinical scenario of therapy resistance [2, 3]. Using these models, we found that residual

resistant disease cells (RR) of GBM acquire transient therapy induced senescence (TIS) and multinucleated giant cells (MNGCs) phenotype and eventually give rise to relapse [2, 3, 4]. Therefore, identifying molecules that drive resistance in residual cells will be of utmost importance for GBM therapeutics.

The 14-3-3 family proteins are involved in cellular processes like intracellular signalling, differentiation, proliferation, transcriptional regulation, cytoskeletal organization, stress signalling, apoptosis, and tumorigenesis [5, 6, 7, 8]. Of the seven isoforms of 14-3-3 protein, 14-3-3ζ plays a pivotal role in regulating multiple signalling pathways in cancer development, progression, and therapy resistance [9, 10, 11]. It is

---

* Corresponding author.
  E-mail address: sdutt@actrec.gov.in (S. Dutt).
[1] These authors share co-first authorship.

known to be overexpressed and associated with poor prognosis in breast, lung, head and neck, and glioblastoma [12]. In glioblastoma, 14-3-3ζ knockdown is shown to induce apoptosis [13]. However, its role in mediating radiation resistance in GBM has not been explored. In this study, we examined the role of 14-3-3ζ in the survival of residual disease cells of GBM and identified novel interacting partners of 14-3-3ζ in residual cells.

2. Materials and methods

2.1. Cell culture and growth conditions

GBM grade IV cell lines U87MG and SF268 were obtained from ATCC and maintained in DMEM (Gibco, USA) containing 10% FBS (HiMedia, India), penicillin (200 U/ml), streptomycin (100 μg/ml) and incubated at 37 °C in a humidified incubator with 5% CO_2. Patient sample (PS) derived short-term primary cultures were grown in DMEM:F12 (Gibco, USA) containing 15% FBS (HiMedia, India) as described previously [2].

2.2. Cell synchronization and radiation treatment

The cells growing in FBS containing media were washed with 1X phosphate-buffered saline (PBS) and incubated with 0.05% FBS containing DMEM for 72 h. After that, cells were grown in media containing 10% or 15% FBS and irradiated using ^{60}Co γ-rays with the following doses- 8 Gy (U87MG), 6.5 Gy (SF268), and 10 Gy (PS2).

2.3. Cell survival and clonogenic assay

Cell survival was monitored by counting viable cells after trypan blue staining every alternative day until 22 days of post-irradiation, as reported previously [2]. For clonogenic assay, cells were irradiated with different doses of radiation (0–10 Gy) following the protocol described earlier [4].

2.4. Quantification of MNGCs formation

The number of MNGCs formation was quantified from the bright-field microscopy images, and DAPI stained images as mentioned earlier [2, 4].

2.5. Beta-galactosidase assay

Senescence was detected using the gold standard beta-galactosidase assay as described earlier [2, 4].

2.6. Transmission electron microscopy

The previously described protocol was followed [14]. Briefly, 10 million cells were washed twice with 1X PBS and fixed with 1 ml of 3% glutaraldehyde (fixative) at 4 °C for 2 h followed by washing with 1 ml of 0.1 M sodium cacodylate buffer. Sections were prepared using an ultra-microtome (Leica UC7, Germany). Sections were contrasted with uranyl acetate and lead citrate. Micrographs were taken under Jeol 1400 plus TEM (Japan) at 120 kV. Mitochondria were analysed from electron micrographs of at least 10 cells per experimental condition. The average number of mitochondria was calculated from two independent biological experiments.

2.7. Quantitative proteomic analysis using iTRAQ to identify differential expression of 14-3-3ζ in RR cells

The differential proteomic analysis to identify 14-3-3ζ was performed using iTRAQ labelling coupled with LC-MS/MS. Nanoflow electrospray ionization tandem mass spectrometric analysis of iTRAQ labelled peptide samples was carried out using LTQ-Orbitrap Velos (Thermo Scientific, Bremen, Germany) interfaced with Agilent's 1200 Series nanoflow LC

system. The MS data were analysed using Proteome Discoverer (Thermo Fisher Scientific, Version 1.4). MS/MS search was carried out using SEQUEST and MASCOT search algorithms against the NCBI RefSeq database (release 52 40) containing 31,811 proteins. Precursor and fragment mass tolerance were set to 20 ppm and 0.1 Da, respectively. False Discovery Rate (FDR) was calculated by searching the proteomic data against a decoy protein database. Only those Peptide Spectrum Matches (PSMs) that qualified for a 1% FDR threshold were considered for further analysis. Unique peptide (s) for each protein identified was used to determine relative protein quantitation based on the relative intensities of reporter ions released during MS/MS fragmentation of peptides. 14-3-3ζ differential expression values were identified from 5 biological replicates [16].

2.8. Western blot analysis

Cells were lysed using EBC lysis buffer (120 mM NaCl, 50 mM Tris-Cl (pH 8.0), 0.5% (v/v) Nonidet P-40, 50 μg/ml PMSF and protease, phosphatase inhibitor cocktail. 40 μg of protein was used for immuno-blotting using anti-14-3-3ζ (rabbit, 1:1000; Pierce cat # PA5-27317) and beta-actin (rabbit, 1:4000 dilution; Pierce) antibodies. Immune-reactive proteins were visualized using an enhanced chemiluminescence (ECL) reagent (Bio-Rad, USA).

2.9. RNA extraction, complementary DNA synthesis, and quantitative PCR

Total RNA was extracted by TRIZOL reagent (Invitrogen) according to the manufacturer's protocol. Complementary DNA was synthesized using the SuperScript III First-Strand kit (Invitrogen) as per the manual instructions. Quantitative PCR was carried out using Roche Light Cycler Master Mix using Light Cycler 480 real-time PCR system. GAPDH was used as an internal control. For mtDNA content analysis, the protocol used by Malik et al was followed [15]. qPCR primer sequences are provided in Supplementary Table 1. Fold changes were calculated using the ΔΔCt method.

2.10. Generation of stable 14-3-3ζ shRNA cell lines

HEK-293FT cells were transfected with pZIP CMV 14-3-3ζ shRNA constructs along with the packaging vector pPAX and helper vector pMD2 using Lipofectamine 3000 (Invitrogen). Viral supernatant was collected at 48 h and 72 h post-transfection and infected in 0.3 $\times 10^6$ SF268 and U87MG cells. Positive clones were selected using 2 μg/ml puromycin.

2.11. Bacterial purification of GST-tagged 14-3-3ζ

Plasmid pGEX-4T encoding glutathione S-transferase (GST)-tagged-14-3-3ζ protein (a kind gift from Dr. Sorab Dalal, ACTREC) was transformed in BL21. The culture was grown until an OD$_{600}$ nm of 0.4–0.6 was reached, followed by growing the culture in the presence of 0.1 mM of IPTG for 3 h. For protein purification, cells were collected and lysed with 1% Triton X –100. The lysate was incubated with glutathione sepharose beads (50% slurry) for 1 h in the cold. The beads were washed thrice with NET-N buffer (20 mM Tris-HCl pH 8, 100 mM NaCl, 0.5 mM EDTA pH 8, 0.5% NP-40) before being suspended in NET-N buffer and stored at 4 °C.

2.12. GST pull-down assay using GST tagged 14-3-3ζ as bait

$10–20 \times 10^6$ cells were lysed using EBC lysis for 45 min on ice. 500 μg of lysate was incubated with 30 μl of glutathione sepharose beads with GST tagged 14-3-3ζ in the NET buffer for 1–2 h at 4 °C. The beads were washed with NET –N buffer 6–7 times and boiled for 5 min in the 2X laemmli buffer, and supernatant was run onto SDS PAGE. The gel was silver stained, and the proteins bands were in-gel digested for protein identification by mass spectrometry.

2.13. Mass spectrometry for identification of 14-3-3ζ interactors

The silver-stained protein bands were excised from the gels and washed with 100 μl of 50 mM ammonium bicarbonate (NH_4CO_3) and 100% acetonitrile in a 1:1 ratio followed by a vacuum drying for 15 min. Next, 200 μl of 10 mM DTT and 50 mM NH_4CO_3 was added in a 1:1 ratio and incubated at 55 °C for 45 min, followed by the addition of 55 mM IAA in 50 mM NH_4CO_3 and incubation for 30 min at room temperature. After washing the gel particles thrice with 200 μl 50mM NH_4CO_3 and acetonitrile (1:1) for 15 min, the gel particles were resuspended in acetonitrile and vacuum dried for 15 min. 10–15 μl of trypsin (10 ng/μl) was added to the vacuum dried particles and incubated at 37 °C overnight. The next day, 100 μl of 0.1% TFA was added, vortexed for 15 min, and the supernatant collected. 100 μl of 0.1% TFA in 50% acetonitrile was added, vortexed, and supernatants collected twice. The peptides obtained post vacuum dry was purified using C-18 columns for desalting. This was done by resuspending the pellet in 20 μl of 0.1% formic acid and washed through C-18 columns equilibrated with 80% acetonitrile. The samples were finally eluted in 60 μl acetonitrile thrice, followed by air-drying and resuspension in 20 μl 0.1% formic acid. 18 μl of the supernatant was collected for mass spectrometry using Nano-LC (ABSCIEX, Eksigent)-ESI-Q-TOF (ABSCIEX, Triple TOF 5600 plus). The MGF files were analysed using Protein Pilot software. Proteins with >95 peptide scores were considered for the analysis. Three biologically independent experiments were performed.

2.14. Statistical analysis

All the data were represented as means ± SD of three independent experiments until it was mentioned in the respective section. The two-tailed Student's t-test was applied for statistical analysis. p-values were denoted as '*' ($0.01 < p \leq 0.05$), '**' ($0.001 < p \leq 0.01$), and '***' ($p \leq 0.001$).

3. Results

3.1. Quantitative proteomic analysis revealed increased expression of 14-3-3ζ in RR cells

We have previously developed an *in vitro* cellular model from clinically relevant primary patient samples and cell lines that recapitulate the clinical scenario of resistance, as illustrated in Figure 1A. In this model, following the treatment of a lethal dose of radiation to the parent culture, we can capture the residual resistant disease cells (RR) that survive radiation and are <10% of the parent population. These RR cells remain transiently non-proliferative and acquire senescent and multinucleated and giant cell (MNGCs) phenotype but eventually overcome senescence and relapse [2]. Here, we first repeated growth kinetics of U87MG and patient sample (PS2) post-irradiation with 8 Gy & 10 Gy, respectively. As seen from Figure 1B, C, the cells initially show proliferation followed by cell death and survival of less than 10% of cells. These cells that survive enter a transient non-proliferative phase followed by resumption of growth forming a relapse population. To gain further knowledge about the unique molecular players influencing the phenotypic and functional characteristics of residual cells, we had earlier generated and analysed quantitative proteomics data from the parent, residual, and relapse cells from our cellular model [16]. Using that data here we report that 14-3-3ζ is significantly up-regulated (>1.5 fold) in residual cells of at least 4 out of the 5 biologically independent experiments performed using SF268 cells. The relative peptide intensities of 14-3-3ζ in residual (RR) cells compared to the parent (P) SF268 cells are shown in Figure 1D. The higher protein expression of 14-3-3ζ in residual cells was further confirmed by western blots of parent (P) and residual (RR) cells of GBM cell lines (SF268 and U87MG) and also in parent and residual cells of the patient sample derived primary culture (PS2) (Figure 1E). Corroboratively, real-time qPCR also revealed up-regulation of 14-3-3ζ transcripts in the RR population of SF268 cell line (Figure 1F).
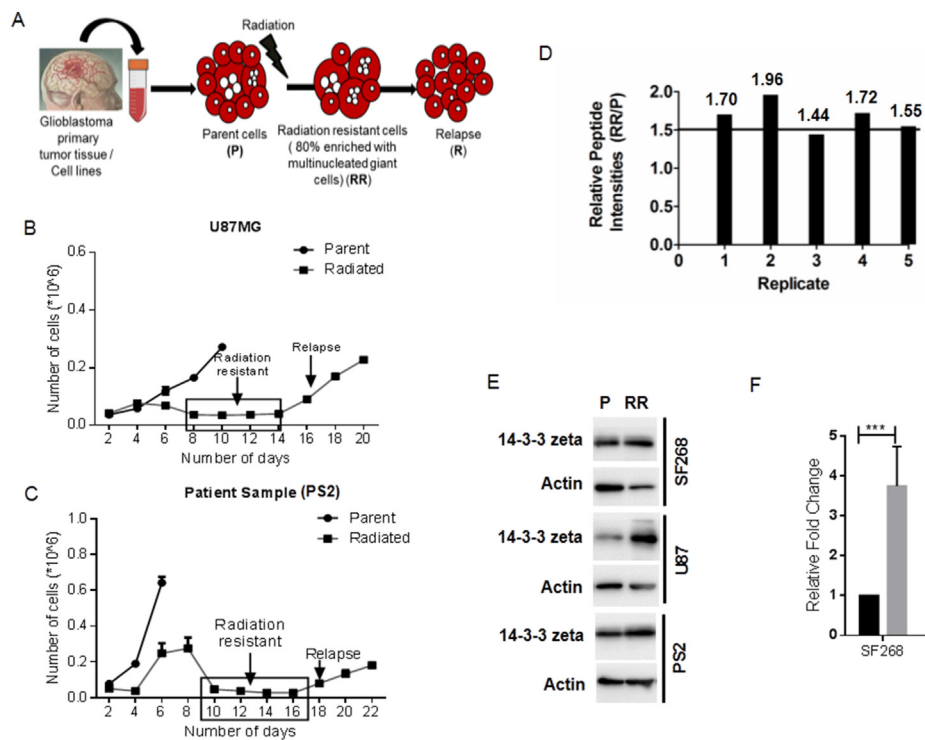
Figure 1. Up-regulation of 14-3-3ζ in residual resistant disease cells. (A) Schematic diagram shows the *in vitro* radiation resistant model of Glioblastoma that captures residual disease cells (RR) as well as recurrent population (R) from the parent (P) population. (B) & (C) Cell proliferation assay using trypan blue staining showing the non-proliferative residual disease cells (radiation-resistant) and relapse in U87MG and patient sample 2 (PS2). (D) Graph shows relative peptide intensities of 14-3-3ζ in SF268 RR cells in five replicates of independent iTRAQ experiments. (E) Representative western blots showing the up-regulation of 14-3-3ζ in the RR cells of SF268, U87MG, and PS2. Beta-actin was used as a loading control (The uncropped original blots are provided as Supplementary Figure 1). (F) Real-time qPCR data showing the fold change of 14-3-3ζ gene expression in SF268 RR cells. Data represent mean ± SD of three independent experiments. *** denotes P ≤ 0.001.

3.2. Reduced cell survival with a concomitant increase in MNGCs formation and radiation-induced senescence after 14-3-3ζ knockdown

To determine the role of 14-3-3ζ in the survival and radiation resistance of residual disease cells, stable clones of shRNA mediated 14-3-3ζ knockdown cells were generated in SF268 and U87MG. The knockdown of 14-3-3ζ was confirmed using the western blot (Figure 2A). Of all the three shRNAs (sh1, sh2, and sh3), cells expressing shRNA3 (sh3) showed maximum knockdown for 14-3-3ζ in both cell lines as compared to the scrambled (Scr), and thus, these cells were used for subsequent experiments. To determine if 14-3-3ζ has a role in the survival of GBM cells to radiation, a clonogenic cell survival assay with different doses (0–10 Gy) of radiation was performed. Knockdown (KD) of 14-3-3ζ radio-sensitized SF268 cells to higher doses of radiation (6 and 8 Gy), as shown in Figure 2B. Clonogenic assay underscores the long-term proliferative potential of cells in terms of colony formation with or without any perturbation. We then argued that such radio-sensitization in 14-3-3ζ KD cells was due to induction of TIS, as depicted in our previous studies, which report transient senescence and MNGC phenotype in RR cells. Therefore, the role of 14-3-3ζ in RR cells in terms of MNGCs formation and senescence induction was examined. Subjecting SF268 sh3 cells to its lethal dose of radiation revealed a significantly higher % of MNGCs in RR (66.53 ± 3.91) population compared to the Scr (44.55 ± 2.10) (Figure 2C). Concurrently, a significant increase in % of beta-gal positive cells was also observed in 14-3-3ζ KD RR (40.93 ± 6.59) cells compared to Scr RR (20.69 ± 5.42) (Figure 2D, E), suggesting increased radiation induced senescence in 14-3-3ζ KD cells.

3.3. 14-3-3ζ negatively regulates mitochondrial biogenesis in RR cells

Since 14-3-3ζ knockdown we found to increase the senescence phenotype of residual cells, we checked if RR cells had elevated metabolic activity. For this, we checked mitochondrial biogenesis. We quantified the mitochondrial numbers using transmission electron microscopy (TEM) and mtDNA content by real-time qPCR. Interestingly, we found that knockdown of 14-3-3ζ did increase the number of mitochondria (59.48 ± 8.86 vs 39.18 ± 3.40 in SF268 and 125.6 ± 10.30 vs 79.40 ± 7.39 in U87MG) as well as the mtDNA content (~3 fold in SF268) in RR cells, indicating increased mitochondrial biogenesis, compared to scr RR cells (Figure 3A, B, C, and D).

3.4. Identification of interacting partners of 14-3-3ζ

In order to identify the molecular players and biological pathways influenced by 14-3-3ζ in the residual GBM cells, especially the metabolic phenotype of RR cells, we performed GST pull down experiments to identify the interacting partners of 14-3-3ζ in the RR cells. For this, GST tagged 14-3-3ζ was expressed and purified from a bacterial system using pGEX 4T 14-3-3ζ vector. Overexpressed protein was run on the SDS PAGE to check for its purity. The identity of the purified protein was confirmed by mass spectrometry (Figure 4A). This purified protein was then incubated with whole cell lysates of SF268 RR and U87MG RR cells, and a GST pull-down assay was performed. The interacting proteins were eluted and resolved on a SDS PAGE (Figure 4B). In-gel trypsin digestion was carried out and run through LC-MS-MS for protein identification.

After combining three biologically independent experiments, 27 proteins were found to interact with 14-3-3ζ in SF268 RR cells, and 34 proteins were found to interact in U87MG RR cells (Supplementary Table 2). A gene set overlap was done using Gene List Venn Diagram online tool to identify common interactors of 14-3-3ζ between SF268 and U87MG with known interactors of 14-3-3ζ (Figure 4C). In total, 15 overlapping proteins were found, of which 9 were novel binding partners, and 5 were known interacting partners of 14-3-3ζ (Figure 4D). A gene set overlap of these 9 novel proteins with interacting partners of other 14-3-3 isoforms
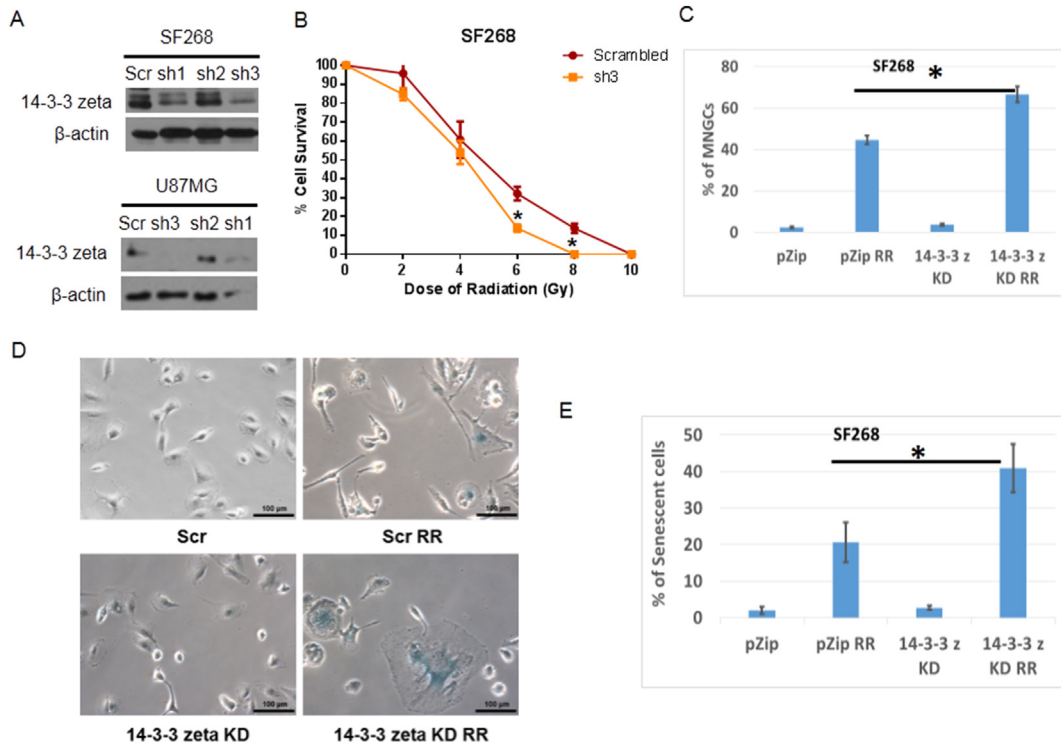
Figure 2. 14-3-3ζ knockdown increases MNGCs formation and radiation-induced senescence in RR cells. (A) Representative western blots showed the stable knockdown of 14-3-3ζ in SF268 and U87MG cells (The uncropped original blots are provided as Supplementary Figure 1). (B) Clonogenic radiation survival of SF268 cells after stable knockdown of 14-3-3ζ (C) Bar diagram depicts the percentage of MNGCs formed in RR population of SF268 after 14-3-3ζ knockdown. (D) Typical images of senescent cells showing beta-gal positivity in SF268 RR cells after 14-3-3ζ knockdown. Scale bar 50 μm. (E) Senescent positive cells were scored and plotted as the percentage of senescent positive cells. Data represent the mean $\pm$ SD of three independent experiments. *denotes P $\leq$ 0.05.
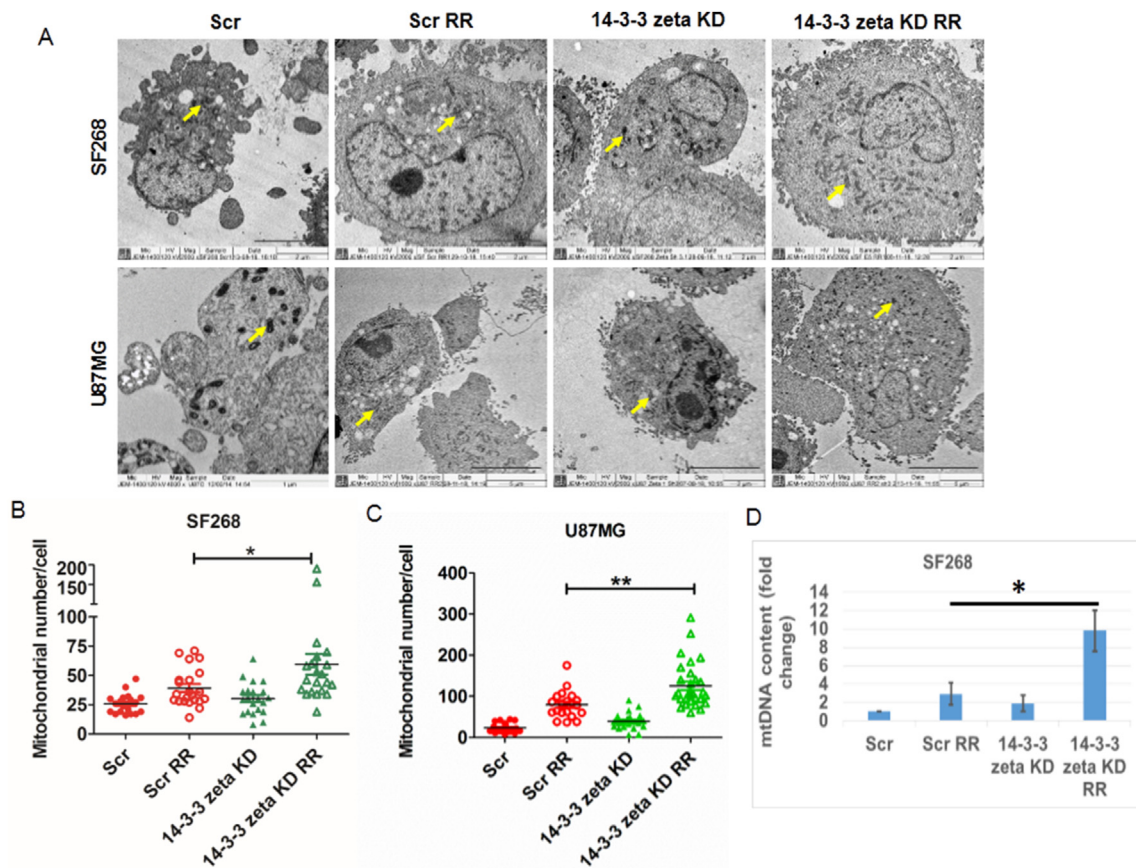
Figure 3. 14-3-3ζ negatively regulates mitochondrial biogenesis in RR cells. (A) Transmission electron micrographs of non-irradiated and RR cells of SF268 and U87MG after 14-3-3ζ knockdown (14-3-3 zeta KD) showing mitochondria (yellow arrows). Cells with scrambled shRNA (Src) are the control. Scale bar 1 μm. (B and C) Dot plot quantifies mitochondrial number per cell of SF268 and U87MG in different conditions, as mentioned. Each data point represents the mean of at least 10 cells from two independent experiments. * denotes P $\leq$ 0.05, ** denotes P $\leq$ 0.01. (D) Graph shows fold change of mitochondrial DNA content in non-irradiated and RR cells of SF268 following 14-3-3ζ knockdown. Data represent mean $\pm$ SD of three independent experiments. * denotes P $\leq$ 0.05.

(ε, γ, σ, β, η, θ) revealed 6 out of 9 novel binding partners as specific interacting partners of 14-3-3ζ. (Supplementary Figure 1). 11 out of the 15 proteins were also identified in our differential proteomic analysis [16], as shown in column 3 of Figure 4D. Interestingly, 33.3% (5/15) of these proteins are involved in cellular metabolism (glycolysis, TCA cycle, and ATP synthesis), while CAT and PRDX2 are known to aid the cells in overcoming oxidative stress (Figure 4E). Collectively, the majority of the 14-3-3ζ interactor proteins (including the novel binding partners) were identified to be involved in cellular metabolism suggesting 14-3-3ζ′s role as a master regulator of cellular metabolism in residual GBM cells.

4. Discussion

14-3-3 proteins are well-known cancer therapeutic targets owing to their central role in regulating various cellular processes such as proliferation, apoptosis, signal transduction, migration, and invasion [6, 17]. For example, it contributes to oncogenic transformation by inhibiting apoptosis, activating signaling pathways that promote growth, and/or sequestering tumour suppressor proteins [9]. In glioblastoma, 14-3-3ζ expression is shown to be a prognostic marker [18]. Studies have also reported a strong association between 14-3-3ζ overexpression with glioma therapy resistance. For instance, Luo et al. showed 14-3-3ζ positive cells having high cell viability, invasion, and resistance to temozolomide [19]. However, there is limited knowledge regarding the role of 14-3-3ζ in residual disease cell survival, especially that of GBM. Our findings demonstrate significant upregulation of 14-3-3ζ in residual resistant cells of GBM that we have shown possess unique molecular signatures and enhanced ability to survive radiation and form relapse [2, 3, 20]. 14-3-3ζ

depletion is reported to inhibit cellular proliferation and enhance apoptosis in glioblastoma [21]. We found that 14-3-3ζ KD in GBM cells makes them radiosensitive. Also, among the seven isoforms, 14-3-3ζ was the only isoform up-regulated in the RR cells in all the biologically independent proteomics data (data not shown). The expression was confirmed by western blots in the RR cells generated from the cell lines and primary cultures of the patient sample.

Another study reported significant induction of senescence phenotype in glioblastoma after 14-3-3ζ depletion [22], which corroborates our findings that show amplified therapy-induced senescence and MNGCs formation in 14-3-3ζ depleted residual disease cells (Figure 2C, D, E). These data highlight the therapeutic opportunity of inducing senescence in GBM by inhibiting 14-3-3ζ. This is the first study in which 14-3-3ζ inversely regulates mitochondrial number as well as mtDNA content in residual disease cells, suggesting a link between 14-3-3ζ mediated mitochondrial biogenesis and GBM therapy resistance.

14-3-3ζ is known to regulate numerous cellular processes via interaction with various proteins [23]. 14-3-3ζ also serves as a hub for several key protein-protein interactions (PPI) involved in tumorigenesis. For example, 14-3-3ζ binds to Akt-phosphorylated Bad, a pro-apoptotic protein, thereby blocking the inhibition of Bcl-2, an anti-apoptotic protein leading to increase proliferation of the tumour [24]. Similarly, 14-3-3ζ and β negatively regulates the tuberous sclerosis complex (TSC1 and TSC2) tumour suppressor gene product, tuberin, thus, compromising the ability of the TSC1-TSC2 complex to reduce S6K phosphorylation [25, 26]. In fact, bio-grid database analysis shows that 14-3-3ζ interact with approximately 620 proteins. Therefore, we reasoned that the inverse relationship that we report in this manuscript between 14-3-3ζ and mitochondrial biogenesis in
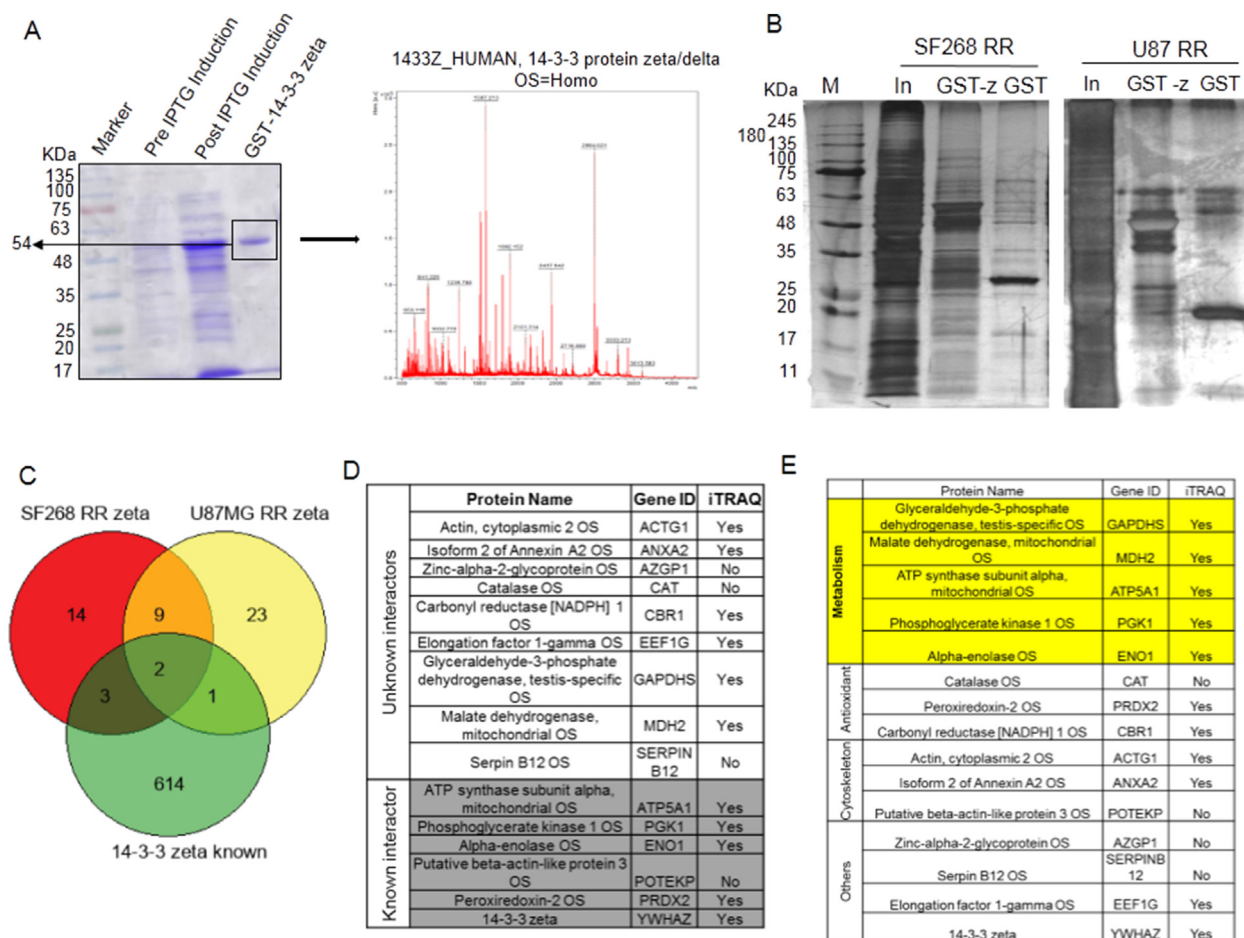
Figure 4. Identification of 14-3-3ζ interacting partners in RR cells. (A) Coomassie stained SDS-PAGE gel showing the bacterial over-expression of GST-tagged 14-3-3ζ protein (left panel) followed by purification and confirmation by mass spectrometry (right panel). (B) The silver stained gel shows the interacting partners of the GST pull-down experiment of recombinant 14-3-3ζ protein incubated with RR cell lysate of SF268 and U87MG. M (marker), In (input), GST-z (GST-14-3-3ζ), GST (vector alone) (C) Venn diagram shows the overlap of 14-3-3ζ interactors identified from RR population with the known interactors. (D) List of 14-3-3ζ interactors identified from the GST-14-3-3ζ pull down experiments and proteins identified in an independent iTRAQ experiment from our lab [18]. (E) Functional classification of 14-3-3ζ interactors.

residual disease cells of GBM is mediated by its PPI. However, there are no reports of 14-3-3ζ interacting partners in GBM residual disease cells. Thus, we performed *in vitro* GST pull-down assay to identify interacting partners of 14-3-3ζ in the RR cells of SF268 and U87MG. Our study identified 15 proteins as 14-3-3ζ interactors in the GBM RR population, out of which 9 are novel partners (Figure 4D). Further, we found that 5 of the identified proteins were enzymes involved in metabolisms, such as glycolysis (GAPDH, PGK1, ENO1), TCA cycle (MDH2), and ATP synthesis (ATP5A1). The 14-3-3 proteins have been shown to regulate cellular metabolism [27]. 14-3-3 ζ deficiency is linked with the increased mitochondrial respiratory reserve in platelets regulating its bioenergetics [28]. In another study, quantitative proteomic analysis of mitochondria from sensitive and resistant ovarian cancer cells also identified 14-3-3ζ to be differentially present in the mitochondria of resistant cells [29]. Therefore, the identification of metabolic enzymes as 14-3-3ζ interacting partners and antioxidants such as CAT and PRDX2 indicate that 14-3-3ζ might regulate the cellular metabolism in RR cells of GBM to help them survive the radiation stress.

Although there are no clinically approved drugs targeting 14-3-3ζ, its role in regulating versatile biological pathways has established it as a potential drug target class. Several groups are working towards developing peptide and peptidomimetic *in vitro* inhibitors of 14-3-3s. For example, difopein (dimeric R18 peptide inhibitor of 14-3-3s) was shown to disrupt 14-3-3 interactions and sensitized cultured cells to cisplatin-induced apoptosis [30]. Further difopein was also shown to inhibit the growth of xenografted glioma cells in mice [31]. Thus, it established

a proof of concept for targeting 14-3-3s *in vivo*. Other current therapeutic interventions related to 14-3-3s are based on the targeting PPI by developing small molecule modulators that either inhibit (like compound 2–5, BV02, FOBISIN101) or stabilize (like Fusicoccin A, Pyrrolidone 1, Epibestatin) PPI [32]. These small molecules serve as tool compounds to study the 14-3-3 chemical biology and therapeutic discovery. Although the functional overlap between different isoforms of 14-3-3s, targeting specifically ζ isoform is a challenge. However, given that six out of the nine novel interactors found in our study are specific binding partners for 14-3-3ζ that did not overlap with any of the interacting partners of other 14-3-3 isoforms (Supplementary Figure 2). Disruption of these interactions should give a 14-3-3ζ specific phenotype, thus highlighting the importance of these findings. Furthermore, an increasing number of 14-3-3s interactors has advanced the 14-3-3 chemical biology by describing the common structural sequences in the interactors as defined as 14-3-3 protein recognition motifs (both canonical and alternative) [9]. We searched the canonical 14-3-3 binding sites in the nine novel interactors that we found in this study using Eukaryotic Linear Motif (ELM) database [33]. We observed that all the interactors had the canonical 14-3-3 binding sites (Supplementary Table 3) strongly supporting our MS data. Further validation and mechanistic studies of the 14-3-3ζ interacting partners will provide insights into several interesting and targetable cellular pathways mediated by 14-3-3ζ in facilitating the survival of residual disease and emergence of recurrence in GBM.

Declarations

Data availability statement

Data included in article/supplementary material/referenced in article.

Declaration of interests statement

The authors declare no conflict of interest.

Additional information

Supplementary content related to this article has been published online at https://doi.org/10.1016/j.heliyon.2021.e08371.

References

[1] B. Oronsky, T.R. Reid, A. Oronsky, et al., A review of newly diagnosed glioblastoma, Front. Oncol. 10 (2021) 574012.

[2] E. Kaur, J. Rajendra, S. Jadhav, et al., Radiation-induced homotypic cell fusions of innately resistant glioblastoma cells mediate their sustained survival and recurrence, Carcinogenesis 36 (6) (2015) 685–695.

[3] E. Kaur, J.S. Goda, A. Ghorai, et al., Molecular features unique to glioblastoma radiation resistant residual cells may affect patient outcome - a short report, Cell. Oncol. (Dordr.). 42 (1) (2019) 107–116.

[4] A. Ghorai, T. Mahaddalkar, R. Thorat, S. Dutt, Sustained inhibition of PARP-1 activity delays glioblastoma recurrence by enhancing radiation-induced senescence, Cancer Lett. 490 (2020) 44–53.

[5] X. Yang, W. Cao, L. Zhang, et al., Targeting 14-3-3zeta in cancer therapy, Cancer Gene Ther. 19 (3) (2012) 153–159.

[6] D.K. Morrison, The 14-3-3 proteins: integrators of diverse signaling cues that impact cell fate and cancer development, Trends Cell Biol. 19 (1) (2009) 16–23.

[7] M. Saline, L. Badertscher, M. Wolter, et al., AMPK and AKT protein kinases hierarchically phosphorylate the N-terminus of the FOXO1 transcription factor, modulating interactions with 14-3-3 proteins, J. Biol. Chem. 294 (35) (2019) 13106–13116.

[8] Y. Gan, F. Ye, X.X. He, The role of YWHAZ in cancer: a maze of opportunities and challenges, J. Cancer 11 (8) (2020) 2252–2264.

[9] C.L. Neal, D. Yu, 14-3-3ζ as a prognostic marker and therapeutic target for Cancer, Expert Opin. Ther. Targets 14 (12) (2010) 1343–1354.

[10] R. Liang, X.Q. Chen, Q.X. Bai, et al., Increased 14-3-3ζ expression in the multidrug-resistant leukemia cell line HL-60/VCR as compared to the parental line mediates cell growth and apoptosis in part through modification of gene expression, Acta Haematol. 132 (2) (2014) 177–186.

[11] Y. Li, L. Zou, Q. Li, et al., Amplification of LAPTM4B and YWHAZ contributes to chemotherapy resistance and recurrence of breast cancer, Nat. Med. 16 (2) (2010) 214–218.

[12] A. Matta, K.W. Siu, R. Ralhan, 14-3-3 zeta as novel molecular target for cancer therapy, Expert Opin. Ther. Targets 16 (5) (2012) 515–523.

[13] M. Hashemi, A. Zali, J. Hashemi, et al., Down-regulation of 14-3-3 zeta sensitizes human glioblastoma cells to apoptosis induction, Apoptosis 23 (11-12) (2018) 616–625.

[14] S. Salunkhe, S.V. Mishra, J. Nair, et al., Inhibition of novel GCN5-ATM axis restricts the onset of acquired drug resistance in leukemia, Int. J. Cancer 142 (2018) 2175–2185.

[15] A.N. Malik, R. Shahni, A. Rodriguez-de-Ledesma, et al., Mitochondrial DNA as a non-invasive biomarker: accurate quantification using real time quantitative PCR without co-amplification of pseudogenes and dilution bias, Biochem. Biophys. Res. Commun. 412 (1) (2011) 1–7.

[16] J. Rajendra, K.K. Datta, S.B. Ud Din Farooqee, et al., Enhanced proteasomal activity is essential for long term survival and recurrence of innately radiation resistant residual glioblastoma cells, Oncotarget 9 (45) (2018) 27667–27681.

[17] J. Li, H. Xu, Q. Wang, et al., 14-3-3ζ promotes gliomas cells invasion by regulating Snail through the PI3K/AKT signalling, Cancer Med. 8 (2) (2019) 783–794.

[18] X. Yang, W. Cao, J. Zhou, et al., 14-3-3ζ positive expression is associated with a poor prognosis in patients with glioblastoma, Neurosurgery 68 (4) (2011) 932–938.

[19] Z. Luo, X. Yang, L.T. Ma, et al., 14-3-3zeta positive cells show more tumorigenic characters in human glioblastoma, Turk. Neurosurg. 26 (6) (2016) 813–817.

[20] E. Kaur, A. Sahu, A.R. Hole, et al., Unique spectral markers discern recurrent Glioblastoma cells from heterogeneous parent population, Sci. Rep. 6 (2016) 26538.

[21] X. Yang, W. Cao, X. Wang, et al., Down-regulation of 14-3-3zeta reduces proliferation and increases apoptosis in human glioblastoma, Cancer Gene Ther. 27 (6) (2020) 399–411.

[22] J.J. Lee, J.S. Lee, M.N. Cui, et al., BIS targeting induces cellular senescence through the regulation of 14-3-3 zeta/STAT3/SKP2/p27 in glioblastoma cells, Cell Death Dis. 5 (11) (2014) e1537.

[23] K.L. Pennington, T.Y. Chan, M.P. Torres, J.L. Andersen, The dynamic and stress-adaptive signaling hub of 14-3-3: emerging mechanisms of regulation and context-dependent protein-protein interactions, Oncogene 37 (42) (2018) 5587–5604.

[24] J. Zha, H. Harada, E. Yang, et al., Serine phosphorylation of death agonist BAD in response to survival factor results in binding to 14-3-3 not BCL-X(L), Cell 87 (4) (1996) 619–628.

[25] M. Nellist, M.A. Goedbloed, C. de Winter, et al., Identification and characterization of the interaction between tuberin and 14-3-3zeta, J. Biol. Chem. 277 (42) (2002) 39417–39424.

[26] S.D. Shumway, Y. Li, Y. Xiong, 14-3-3beta binds to and negatively regulates the tuberous sclerosis complex 2 (TSC2) tumor suppressor gene product, tuberin, J. Biol. Chem. 278 (4) (2003) 2089–2092.

[27] R. Kleppe, A. Martinez, S.O. Døskeland, J. Haavik, The 14-3-3 proteins in regulation of cellular metabolism, Semin. Cell Dev. Biol. 22 (7) (2011) 713–719.

[28] S.M. Schoenwaelder, R. Darbousset, S.L. Cranmer, et al., 14-3-3ζ regulates the mitochondrial respiratory reserve linked to platelet phosphatidylserine exposure and procoagulant function, Nat. Commun. 7 (2016) 12862.

[29] M. Chen, H. Huang, H. He, et al., Quantitative proteomic analysis of mitochondria from human ovarian cancer cells and their paclitaxel-resistant sublines, Cancer Sci. 106 (8) (2015) 1075–1083.

[30] S.C. Masters, H. Fu, 14-3-3 proteins mediate an essential anti-apoptotic signal, J. Biol. Chem. 276 (48) (2001) 45193–45200.

[31] W. Cao, X. Yang, J. Zhou, et al., Targeting 14-3-3 protein, difopein induces apoptosis of human glioma cells and suppresses tumor growth in mice, Apoptosis 15 (2) (2010) 230–241.

[32] J. Zhao, C.L. Meyerkord, Y. Du, et al., 14-3-3 proteins as potential therapeutic targets, Semin. Cell Dev. Biol. 22 (7) (2011) 705–712.

[33] M. Kumar, M. Gouw, S. Michael, et al., ELM-the eukaryotic linear motif resource in 2020, Nucleic Acids Res. 48 (D1) (2020) D296–D306.